Asian Journal of Physics
Vol. 32, Nos 3 & 4 (2023) 211-216
Available on: www.asianjournalofphysics.com

ap

X-ray micro-CT for morphology analysis of ant's head

D Marcos[1,2], P Gómez del Campo[1,5], S Arganda[3], J Montero[3], A Belarra[1,5], T Alieva[4] and M Chevalier[1,5]

[1]*Unidad de Física Médica, Facultad de Medicina, Universidad Complutense de Madrid, Plaza de Ramón y Cajal S/N, Spain*

[2]*Grupo de Ingeniería Biomédica, Universidad de Valladolid, Spain Complutense University of Madrid, 28040 Madrid, Spain*

[3]*Departamento de Biología y Geología, Física y Química Inorgánica, Universidad Rey Juan Carlos, Spain.*

[4]*Facultad de Ciencias Físicas, Universidad Complutense de Madrid, Avda. Complutense S/N, Spain*

[5]*Laboratorio de Micro-CT-UCM, Spain*

Dedicated to Prof Jay M Enoch

Micro-computed X ray tomography is a useful tool for the analysis of internal structure of small animals, including insects. Here, we evaluate the conditions which are optimal for the study of ant´s head morphology by using microfocus X-ray laboratory setup. We demonstrate that it is possible to clearly observe the 3D structure of the ant's head, such as muscles, scalps or antennas, with micrometric resolution. However, fine information about the internal structure (brain), even using staining, is very difficult to obtain using the polychromatic X ray source applied in this study. Segmentation methods allow to extract only global characteristics of the brain: Identifying its volume, brain lobes, oesophagus, pedunculae and subesophageal zone.

Keywords: Electromagnetic radiation, Propagation, Photons, Eye vision mechanism.

1 Introduction

Prof Jay Enoch is one of the pioneers of the biological optics. In this article, devoted to his tribute, we consider the application of X ray radiation to analyze biological objects. Micro-computed tomography (micro-CT) imaging is nowadays widely used in many fields such as electronics, material science, geology, dentistry or biomedicine due to its non-destructive nature that provides 3D information of internal structures in the range of the micrometer. This technique has been recently applied to studies of insects and other small animals [1-3]. In this study, we evaluate different experimental conditions for image acquisition of micro-CT in insects using a polychromatic X-ray source. In particular, we analyze the internal structures of stained ant heads (1-2 mm size), for a quantitative study of anatomical modification of vital organs such as the brain. The study forms part of more general research program focused in increasing the knowledge about neuroanatomical variations in social insects and about the role of nutrition in the defense against disease considering energetic trade-offs between nervous, digestive, and immune systems. The particular characteristics of the size and attenuation properties of insects like ants requires previous research for optimization of imaging conditions. This research plays a crucial role towards automatization of measurements, reconstruction, and analysis of serial samples. In addition, post-processing techniques such as segmentation are also needed to obtain separate information of the ant's internal organs.

Corresponding author
e mail: chevalie@ucm.es (M Chevalier)

2 Material and methods

The in-house designed bench-top micro-CT setup used for this study, see Fig 1, is composed of micro-focus X-ray tube (Hamamatsu, L10951-04 model), multi-axis system including a rotation stage with sample holder and a Hamamatsu AA60 detector. The focus size varies with the X-ray power emission from 20 µm (7 W) to 130 µm (50 W). The AA60 device is composed of scintillator (P43) coupled to a projection optical system (magnification 0.48) equipped with ORCA FLASH 4 (Hamamatsu) camera. The AA60 detector has a pixel size of d =13.6 µm. The position of the X-ray tube is fixed and the source to detector distance (SDD) varies by moving the detector platform in the range from 25 to 2000 mm. Different magnifications are obtained by varying the source to object distance (source-object distance, SOD) for a fixed detector position. Programmable control of the sample holder axial position allows choosing proper imaging conditions.

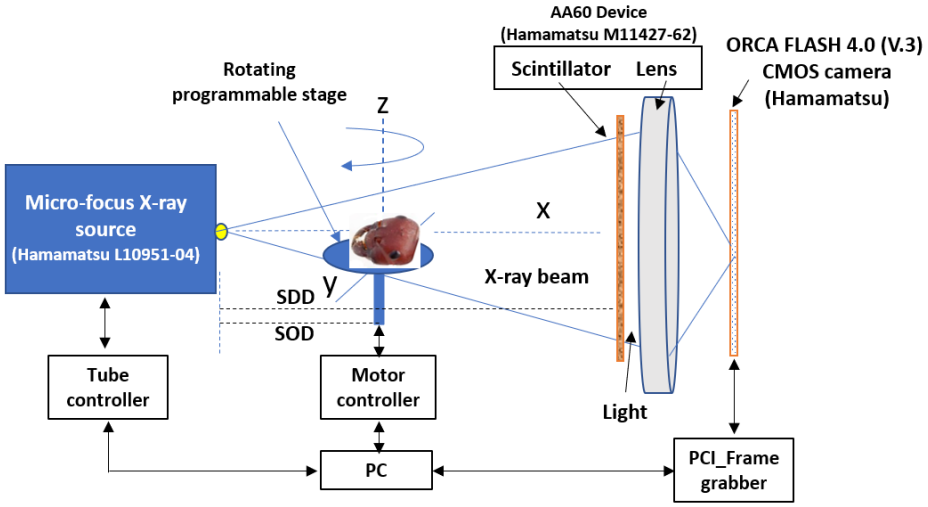

Fig 1. Micro-CT setup.

Heads of Cataglyphis ants were used in this study. The heads were stained by immersion in 1% (Ant 1) and 0.5% (Ant 2) phosphotungstic acid (PTA) solution (1 mg/ml concentration in 70% ethanol) during 20h at room temperature.

The tomograms of the ant heads were acquired in air at SDD = 300 mm, 45 kV and two exposure integrations. The scan range employed in all the scan acquisitions was 360º. Different exposure conditions (Table 1) have been considered. We have studied the impact of several parameters (number of projections, X-ray filtration and staining concentration) on the visualization of the structures of the ant head. The acquired projections have been corrected using the flat field and dark field images. The employed reconstruction algorithm was the Filtered Back Projection (FBP) algorithm included in the Octopus reconstruction software (FDK for cone beam modality).

3 Results and Discussions

The main reason for sample staining is a visualization of soft tissues, in particular the ant´s brain. While for example ant´s head capsule, jaw and muscles are well distinguished without staining, it is not the case for the brain. As an example, 3D rendering of ant´s head for two different staining conditions are shown in Fig 2. As it was expected, the staining concentration was the parameter with a major influence on the visualization of the structures of the ant´s head. Muscles and optical lobes are more clearly depicted when the concentration is high (Fig 2a, c). However, a lower concentration reduces the artefacts due to

x-rays scattering caused by the stain that blur the ant´s brain image as it can be seen by comparing Fig 2c and Fig 2d. This makes it possible to distinguish between different structures into brain (Fig 2d).

Table 1. Micro-CT scanner parameters: Source-object distance (mm), tube loading (μA), focus size (FS), beam filtration (Filter), number of projections (N. Proj), effective pixel size (P. eff) and exposure time. SDD = 300mm, 45 kV, two exposure integrations, and scan range of 360º for all the cases.

Ant (exposure conditions)	SOD (mm)	I (μA)	FS (μm)	Filter	N. Proj.	P. eff (μm)	Exp. Time (s)
1a	150	120	20	--	1000	6,5	3
1b	150	120	20	--	2000	6,5	3
1c	85	120	20	--	2000	3,7	3
1d	85	120	20	0,1 mm Al	2000	3,7	3
2a	85	150	22	0,1 mm Al	2000	3,7	4
2b	85	150	22	--	2000	3,7	4
2c	85	120	22	--	2000	3,7	4

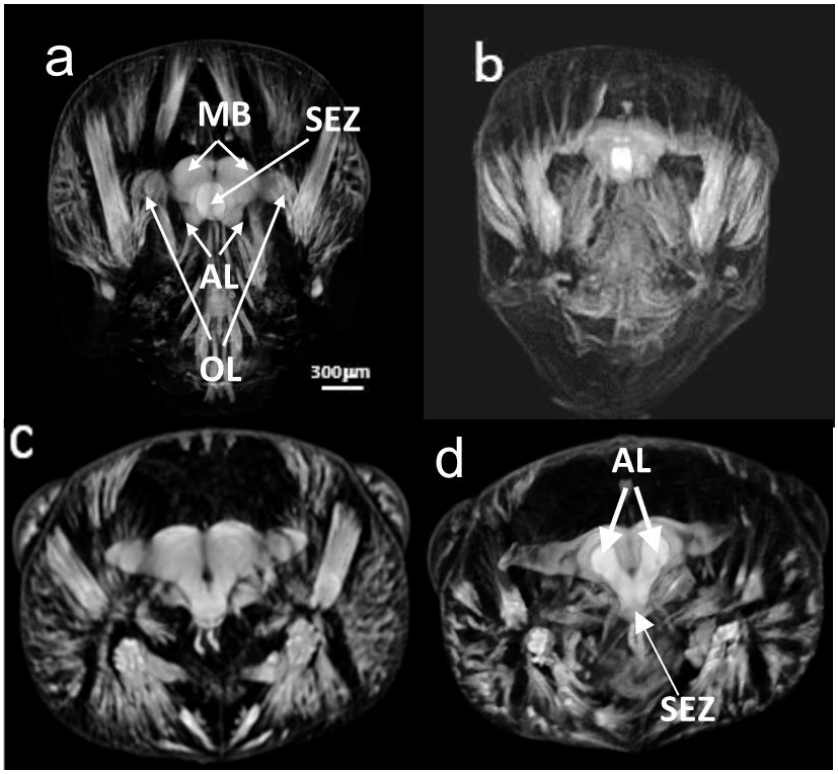

Fig 2. 3D views of ant´s heads for 1% PTA concentration (a, c) and 0.5% PTA concentration (b, d). Abbreviations: MB, mushroom bodies; OL, optic lobes; AL, antennal lobes; SEZ, subesphageal zone.

To evaluate the impact of the different experimental conditions (Table 1) and corrections (rings, spots, etc.) for 3D reconstruction, we have calculated the contrast noise ratio (CNR) at the brain lobe regions in the image slices. The CNR was defined as (MPVL−MPVBG)/STDBG, where MPV is the mean pixel value associated to the regions of interest (ROI) positioned over the brain lobes and the background (see Fig 3), STD represents the standard deviation, and L and BG subindexes stand for brain lobe and

background, respectively. ROI size was adapted to brain lobe sizes in the slices. CNR values for different conditions are shown in Table 2.

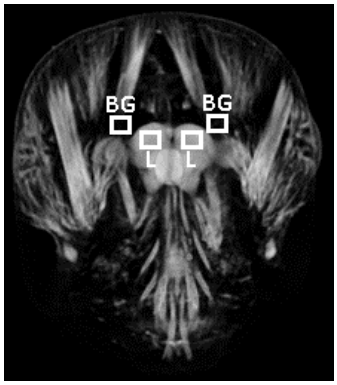

Fig 3. ROI positions for CNR calculations. L and BG abbreviations stand for brain lobe and background, respectively.

Table 2. Average CNR measurements comparing different acquisition conditions and reconstruction parameters.

Parameter	Ant	Parameter value	CNR
N. Proj.	1a	1000	18
	1b	2000	23
P. eff.	1b	6.5	23
	1c	3.7	16
Filter	1c	No	16
	1d	Yes	10
	2b	No	22
	2a	Yes	17
PTA Concentration	1c	1%	16
	2c	0.5%	22

CNR values were considered as a first approach to determine the conditions that provide the optimum slice sets to be used for segmentation techniques and extract valuable ant´s brain information. The CNR increases by around 40% on average when the projection number and the magnification are duplicated. The CNR for acquisitions without interposing an Al filter at the radiation beam output is higher than when a filter was used. By using a filter, the beam is attenuated and its spectrum is changed that produces an increase in the noise of the projections.

Despite having explored the optimal conditions, we could not distinguish the fine structure of the brain because the resolution of the micro-CT system was not high enough. However, several segmentation techniques were tested to extract global information about the ant's brain such as its volume. The applied methods were Thresholding, Splitting and Merging, Region growing, Graph cut [4-6]. Manual segmentation was considered as the reference method (R). The segmentation was applied slice by slice using MatLab [4] and ImageJ software [7]. Figure 4 shows the comparison of one slice brain segmentation using the considered methods. The quantitative comparison of the segmentation methods has been done by calculation of the number of wrong classified pixels: $N_{WC} = |N_M - N_R| / N_M$, where N_M and N_R are the number of pixels belonging to the segmented brain according to the tested method and the manual method that is taken as

the reference [6], respectively. The similarity of the segmentation methods with respect to the reference one is expressed in percentage by: $S = (1 - N_{WC}) \times 100\%$.

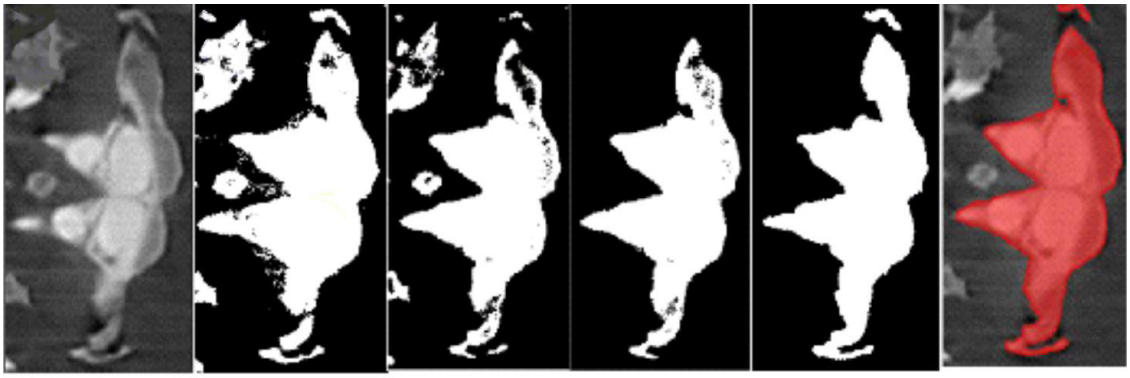

Fig 4. Results of the different segmentation techniques applied to the same slice of the ant's brain.

From the comparison of the S values associated with each segmentation method, we conclude that the most reliable methods for automatic segmentation are the Region growing and Graph cut methods, as shown in Table 3. The analysis also reveals that the segmentation methods provide the best results for dye concentration of 0.5% PTA due to reduction of artifacts in the reconstructed slices of the ant's brain stained with the lower concentration of dye

The volume of the entire ant's head (V_H) and the segmented brain (V_B) (see Fig 5) have been estimated for two ant's heads. We obtained a ratio $V_B/V_H \times 100\%$ of 3.5%.

Table 3. Similarity (S) values for the segmentation methods (M) with respect to the reference (manual segmentation (R)) for the two staining conditions. Experimental conditions for the tomographic acquisitions were 2000 projections and 3.7 μm for the effective pixel. The tube current values were 150 μA and 120 μA for 0.5% PTA and 1% PTA staining concentrations, respectively.

Method	S (%) 0.5% PTA concentration	S (%) 1% PTA concentration
Region growing	88	85
Graph cut	68	83
Thresholding	21	9
Splitting and Merging	4	17

4 Conclusions

We conclude that it is possible to get information about the internal structure of ants´ heads with a resolution of below 10μm. However, this resolution is not sufficient to discriminate the finest structure of the brain. Other relevant aspect is related with the lack of reproducibility of the ant's head positioning in the sample holder. This makes difficult to have similar 3D views of different specimens. Stain concentration plays a pivotal role in the visualization of different structures into the brain. The reconstructed slices are useful to applied segmentation procedures to obtain data about global brain characteristics. The segmentation methods, Region Growing and Graph cut demonstrated the best results that can be used for automatic application.

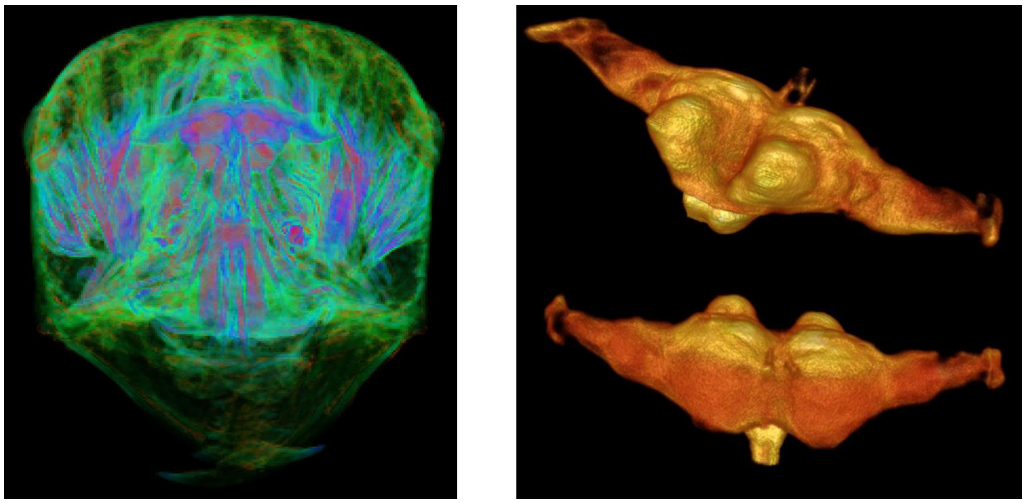

Fig 5. 3D views of the entire ant´s heads (left), brain segmented (right).

Acknowledgments

The Spanish Ministerio de Ciencia y Universidades is acknowledged for the projects PGC2018-095595-B-I0 (DM, AB, TA, and MC) and PGC2018-101012-A-I00 (JM and SA). The Community of Madrid is acknowledged for the founding received by SA in the program "Atracción del Talento Investigador". PGC and AB were under contract (Youth Employment Plan) of the Community of Madrid during the development of this investigation.

References

1. Martín-Vega D, Garbout A, Ahmed F, Wicklein M, Goater C P, Colwell D D, Hall M J R, 3D virtual histology at the host/parasite interface: visualisation of the master manipulator, Dicrocoelium dendriticum, in the brain of its ant host, *Sci Reps*, 8(2018)8587; doi.org/10.1038/s41598-018-26977-2.
2. Poinapen D, Konopka J K, Umoh J U, Norley C J D, McNeil J N, Holdsworth D W, Micro-CT imaging of live insects using carbon dioxide gas-induced hypoxia as anesthetic with minimal impact on certain subsequent life history traits, *BMC Zool*, 2(2017)9; doi.org/10.1186/s40850-017-0018-x.
3. Holdsworth D W, Thornton M M, Micro-CT in small animal and specimen imaging, *Trends Biotechnol*, 20(2002) S34-S39.
4. Woods R E, Eddins S L, Gonzalez R C, (Digital Image Processing using Matlab, Upper Saddle River, NJ : Pearson/ Prentice Hall), 2004.
5. Zhang L, Zhang D, Peng B, A survey of graph theoretical approaches to image segmentation, *Pattern Recognit*, 46(2013)1020–1038.
6. Mirslav Benes B Z, Performance evaluation of image segmentation algorithms on microscopic image data, *J Microsc*, 257(2015)65–85.
7. ImageJ tutorial https://imagej.net/ij/docs/guide/ on-line.

[*Received*: 16.04.2023; *accepted*: 22.04.2023]